

Data-Driven Optimization for Deposition with Degradable Tools

Tony Zheng*, Monimoy Bujarbaruah*, Francesco Borrelli*

* *University of California, Berkeley, CA 94720 USA*
(e-mail:{tony_zheng, monimoyb, fborrelli}@berkeley.edu).

Abstract: We present a data-driven optimization approach for robotic controlled deposition with a degradable tool. Existing methods make the assumption that the tool tip is not changing or is replaced frequently. Errors can accumulate over time as the tool wears away and this leads to poor performance in the case where the tool degradation is unaccounted for during deposition. In the proposed approach, we utilize visual and force feedback to update the unknown model parameters of our tool-tip. Subsequently, we solve a constrained finite time optimal control problem for tracking a reference deposition profile, where our robot plans with the learned tool degradation dynamics. We focus on a robotic drawing problem as an illustrative example. Using real-world experiments, we show that the error in target vs actual deposition decreases when learned degradation models are used in the control design.

Keywords: Autonomous robotics systems, Data-driven optimal control, Modeling.

1. INTRODUCTION

Robotic manipulation in contact-rich tasks have seen great advancements in recent years [Suomalainen et al., 2022]. There has been a push towards robots that can help in daily household chores such as folding clothes [Avigal et al., 2022], wiping surfaces [Leidner et al., 2016], or various kitchen tasks [Ebert et al., 2022]. While these tasks are certainly challenging, there are still unaddressed problems in the field where the contact tool itself changes over time. Examples include cutting blades that decrease in sharpness through repeated use, sandpaper which wears away, or chalk for marking surfaces.

For this work, we consider the deposition with degradable tools in the application of robotic drawing. Artwork and videos generated by AI in recent works [Ramesh et al., 2021, 2022, Villegas et al., 2022, Rombach et al., 2022, Saharia et al., 2022] have been able to produce complex creations that could easily be mistaken as drawn by professional artists. Text-to-image generation has been able to produce some incredible results that allow the user to create highly specific combinations of subjects performing actions in locations, even in the artwork style that they desire [Ramesh et al., 2022, Rombach et al., 2022, Saharia et al., 2022]. Research in predictive language models like GPT-3 [Brown et al., 2020] linked with large image databases [Deng et al., 2009] have been a huge part of these advancements. However, one major hurdle has been translating these artworks into the real world. There are many complex physical interactions involved in various mediums of artwork such as oil painting, pencil sketching,

water-colors, etc. Work has been done the decomposition of images into individual strokes to reproduce the image [Huang et al., 2019, Tong et al., 2021]. The final drawn images can be highly accurate but they lack insight in actually making a robot hold a paintbrush or pencil to produce those strokes. Current state-of-the-art approaches for robotic drawing are predominately hand-tuned open loop sequences with custom end-effectors that make it easier to have a constant force output and frequent reset sequences to allow for consistency [Jain et al., 2015, Kotani and Tellex, 2019]. A more accurate replication of human drawing would take the deformation of a tool-tip into account and change the policy accordingly. To the best of our knowledge, there has not been works that use visual feedback to update the model of a tip’s degradation to produce more accurate strokes.

In this paper, we formulate the deposition task as a model-based constrained finite time optimal control problem, where we model the deposition and the degradation of the tool tip. The parameters of these models are not known a-priori, and we learn these using collected data. We focus on the specific example of a robot sketching using a pencil. The unknown degradation and deposition models of the pencil are parameterized as a function of the applied force and the distance drawn. We present detailed experiments with a UR5-e robot where we show that accounting for the degradation of the tip and planning strokes accordingly improves the sketching quality measured in terms of the difference in stroke width error.

2. RELATED WORK

Simulated stroke generation Reinforcement learning approaches have been shown to work in generating realistic strokes. Xie et al. [2013] formulates brush strokes as an Markov decision process and solves it using policy gradient methods. Huang et al. [2019] takes target images

* This work was supported by ONR-N00014-18-1-2833, NSF-1931853, and AFRI Competitive Grant no. 2020-67021-32855/project accession no. 1024262 from the USDA National Institute of Food and Agriculture. This grant is being administered through AIFS: the AI Institute for Next Generation Food Systems (<https://aifs.ucdavis.edu>).

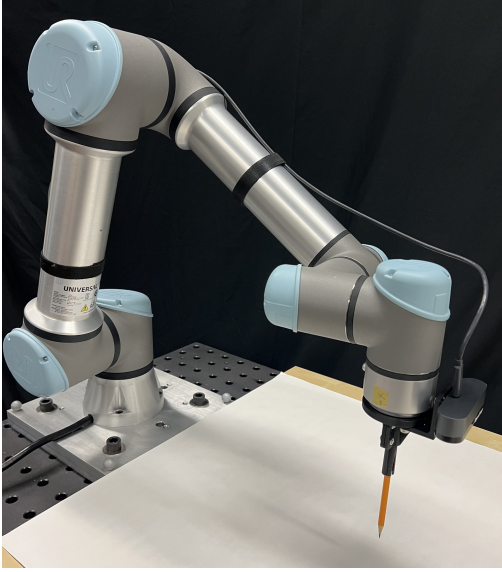


Fig. 1. The considered experimental setup.

and decomposes them into stroke sequences with deep reinforcement learning. Cao et al. [2019] introduced a CNN-based auto-encoder to generate multi-class sketches. Tong et al. [2021] uses the gradient of grayscale values to determine pencil stroke sequences used to recreate images. While these works produce strokes that appear similar to real ones, they are not tested on real robots where the actual deposition will likely differ from their expected.

Real-world stroke generation Wang et al. [2020] formulate calligraphy writing as a trajectory optimization problem and developed a novel dynamic brush model. They produce open-loop trajectories for that a robot can follow but do not close the loop. Lam and Yam [2009] use linear regression to relate brush pressure with actual deposition width and generates trajectories to fill a desired calligraphy image. Bidgoli et al. [2020] trains a generative model on expert artist motion data in order to extract artistic style into robotic painting. They did not include closed-loop control and studied whether a playback of the artist motions with a robotic arm could produce brushstrokes similar to humans. Kotani and Tellex [2019] trains RNNs combined with LSTMs on images and produces commands for the robot that aim to draw strokes in continuous fluid motions. Gao et al. [2020] uses CNNs and GANs to extract sketch outlines from images and replicates the contours with a brush-pen. These actual robot demonstrations are done with open-loop sequences as well.

Adamik et al. [2022] explores pencil drawing and uses genetic algorithms to produce line segment sequences that can reproduce detailed drawings. Their robot uses a passive flexible tool to hold their custom graphite writing implement and compensates for drawing pressure changes over the surface. The tool-tip is designed in such a way that the graphite can be reset and calibrated frequently. Song et al. [2018] uses impedance control to draw on arbitrary surfaces using a pen. O'Dowd [2019] corresponds force values with grayscale values of an image to shade using a pencil. These methods do not consider degradation of the tool-tip over time.

3. PROBLEM FORMULATION

In this section, we describe the models used for our optimization based deposition problem.

3.1 Reference Stroke

When drawing a picture, there are a limitless number of ways to decompose a desired image into individual strokes. We start with the assumption that each reference stroke is already given using stroke generation methods such as [Tong et al., 2021, Huang et al., 2019]. The output of these generators are the parametric curve equations, width along the stroke, and color values. We convert these image coordinates so that the reference states, $s_{\text{ref}}(\zeta(t))$, to be used in the cost function for our optimization problem are:

$$s_{\text{ref}}(\zeta(t)) = \begin{bmatrix} x_{\text{ref}}(\zeta(t)) \\ y_{\text{ref}}(\zeta(t)) \\ W_{\text{ref}}(\zeta(t)) \end{bmatrix}, \quad (1)$$

where t is the time step, $\zeta(t)$ is a parameter used to define the curve s_{ref} , $\{x_{\text{ref}}(\zeta(t)), y_{\text{ref}}(\zeta(t))\}$ are the x and y positions (m) respectively and $W_{\text{ref}}(\zeta(t))$ is the deposition width (m). Visually represented in Fig. 2, $p(\zeta(t))$ is the tangent vector to the stroke reference path $\{x_{\text{ref}}(\zeta(t)), y_{\text{ref}}(\zeta(t))\}$ sampled at any time step. Then, the deposition width $W_{\text{ref}}(\zeta(t))$ is defined as the thickness of the stroke cross section at that point measured in a direction perpendicular to $p(\zeta(t))$. Henceforth, we will replace $(\zeta(t))$ with (t) for the simplicity of notations.

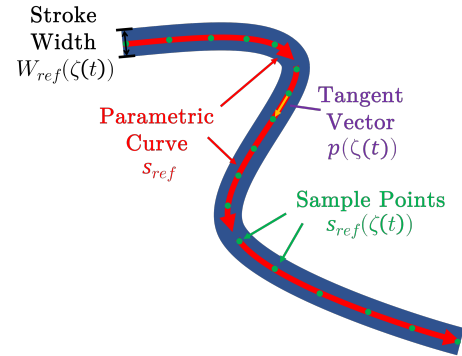


Fig. 2. Stroke Analysis

3.2 End Effector Modeling

We start the modelling of the discretized system beginning with the robot arm. We treat the end-effector of the robot arm as a single integrator:

$$\bar{x}(t+1) = A\bar{x}(t) + Bu(t), \quad (2)$$

with $A = I_4$, $B = dt \cdot I_4$ where I_n denotes the identity matrix of size n , and sampling time $dt = 0.008\text{s}$. The states and inputs are

$$\bar{x}(t) = \begin{bmatrix} x(t) \\ y(t) \\ z(t) \\ \psi(t) \end{bmatrix}, u(t) = \begin{bmatrix} v_x(t) \\ v_y(t) \\ v_z(t) \\ \omega_\psi(t) \end{bmatrix}, s(t) = \begin{bmatrix} x(t) \\ y(t) \\ W(t) \end{bmatrix}, \quad (3)$$

where $\{x(t), y(t), z(t)\}$ are end effector positions. The angle $\psi(t)$ is the angle between the pencil's ellipsoidal cross section's minor axis projected on the xy plane, and

the tangent to the stroke at time t . The inputs are their respective velocities. During control, we impose state and input constraints for the end-effector at all time steps $t \geq 0$ as given by:

$$x(t) \in \mathcal{X}, u(t) \in \mathcal{U}, \quad (4)$$

for all $t = 0, 1, \dots, N$, where $N > 0$ is the task horizon, and the sets $\{\mathcal{X}, \mathcal{U}\}$ are polytopes.

As the tool is pushed deeper along the z -axis into the surface, a greater force is applied which we model in the following section.

3.3 Force Map Modeling

The force applied by the tool to the work surface can be modeled as a general nonlinear function

$$F(t) = f_F(z(t) - z_{\text{ref}}(t), \eta(t)), \quad (5)$$

where z_{ref} is the work surface height, $z(t) - z_{\text{ref}}(t) \leq 0$ ensures that the tool is penetrating into the surface (for a downward direction), and $\eta(t)$ is a parameter that describes other contact conditions such as soft or dissipative contact. To obtain this relationship, we control the robot such that the tool tip makes contact with the work surface and then applies various penetration depths while taking force measurements. Because the actual function $f_F(\cdot, \cdot)$ is unknown for our tool, we fit a simplified linear model of the form shown below, ignoring the dependence on $\eta(t)$:

$$F(t) = \theta(z(t) - z_{\text{ref}}(t)) + \theta_0, \quad (6)$$

where parameters θ, θ_0 are unknown and to be learned from collected data.

For drawing tools such as pencils, the contact force has a large effect on the rate at which the tip degrades. Our main contribution is that we utilize tip degradation of a rotated tip into the trajectory planning which we model in the next section.

3.4 Tool Tip Modeling

First, we model the pencil tip as a cone which will come into contact with a planar surface as shown in Fig. 3. This

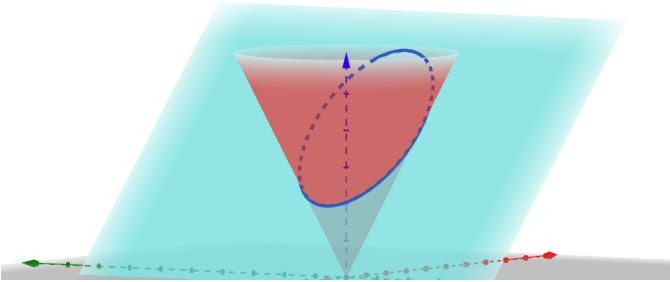


Fig. 3. Intersection of a cone and hyperplane.

results in the general equation for the ellipse:

$$\frac{(m^2 - a^2)^2(x + \frac{ad}{a^2 - m^2})^2}{m^2 d^2} + \frac{(m^2 - a^2)y^2}{d^2} = 1, \quad (7)$$

where m is the slope of the cone, a is the slope of the hyperplane, and d is the vertical offset of the hyperplane from the cone's tip.

Assumption 1. The slope (a) remains the same throughout the task duration to ensure that the shape of the surface stays an ellipse. This also relies on an upper bound for d such that it does not make the hyperplane intersect past the top of the cone.

Under Assumption 1, the intersection formed is an ellipse under the condition that the angle of the plane is shallower than the slope of the pencil's edge, i.e., $|a| < |m|$. We thus have:

$$\alpha(t) = \frac{2m\sqrt{1+a^2}d(t)}{m^2 - a^2}, \quad \beta(t) = \frac{2d(t)}{\sqrt{m^2 - a^2}}, \quad (8)$$

where $\{\alpha(t), \beta(t)\}$ are the major and minor axes of the elliptical cross section at t , respectively. We define the angle γ such that $a = \tan(\gamma)$ which physically describes the angle in which the pencil tip is oriented against the surface. Note that when $\gamma = 0$, the pencil is pointed downward into a horizontal surface which is the perpendicular direction and $\alpha = \beta$.

3.5 Degradation Modeling

The degradation of the tip is modeled as function of the current state of the tip, force applied to the surface with the tip, and distance travelled while in contact. The evolution dynamics of the pencil tip can be described using d from (7):

$$d(t+1) = d(t) + K_d F(t) \left\| \begin{bmatrix} x(t+1) \\ y(t+1) \end{bmatrix} - \begin{bmatrix} x(t) \\ y(t) \end{bmatrix} \right\|_2 \quad (9)$$

where K_d is a scaling parameter. As the pencil is being used and wearing away, the hyperplane is pushed further into the cone.

3.6 Deposition Modeling

Using the geometry of the ellipse, we model this deposition width as:

$$W(t) = \max(\alpha(t) \cos(\psi(t)), \beta(t) \sin(\psi(t))), \quad (10)$$

thus the deposition width is the maximum between the major and minor axes projections measured perpendicular to the stroke at t .

4. DATA-DRIVEN CONTROL SYNTHESIS

In this section, we formulate our data-driven optimization approach for deposition with a degradable tool. Since the parameters from (6) in the degradation (9) models are unknown, we estimate them using data from repeated strokes, *before* attempting to track the reference stroke with the pencil. This is done during a training phase.

4.1 Learning Parameters during the Training Phase

We can rewrite (6) as:

$$F(t) = \mathbf{z}^\top(t) \Theta, \quad (11)$$

where $\mathbf{z}(t) = [z(t) - z_{\text{ref}}(t), 1]^\top$ and $\Theta = [\theta, \theta_0]^\top$. In this case, the estimated parameters $\hat{\Theta}$ can be obtained using ordinary least squares as:

$$\hat{\Theta} = (\mathbf{Z}^\top \mathbf{Z})^{-1} \mathbf{Z}^\top \mathbf{F}, \quad (12)$$

where

$$\mathbf{Z} = \begin{bmatrix} z(0) - z_{\text{ref}}(0) \\ z(1) - z_{\text{ref}}(1) \\ \vdots \\ z(T_{\text{off}}) - z_{\text{ref}}(T_{\text{off}}) \end{bmatrix}, \quad \mathbf{F} = \begin{bmatrix} F(0) \\ F(1) \\ \vdots \\ F(T_{\text{off}}) \end{bmatrix},$$

where $T_{\text{off}} \gg 0$ is the offline time used to collect data and fit the models. We then use $\hat{\Theta}$ in our optimal stroke design. Note that after learning the parameters offline, we assume the pencil is sharpened to its initial state again, so that the given reference stroke can now be tracked using our best parameter estimates $\hat{\Theta}$.

4.2 Optimal Stroke Tracking Synthesis

Let $\hat{\theta}$ and $\hat{\theta}_0$ be our estimates of unknown parameters θ and θ_0 , respectively, obtained offline. The optimal control problem solved at $t = 0$ is given by:

$$\begin{aligned} \min_{U_t} \quad & \sum_{t=0}^N (s(t) - s_{\text{ref}}(t))^T Q (s(t) - s_{\text{ref}}(t)) \\ \text{s.t.,} \quad & \bar{x}(t+1) = A\bar{x}(t) + Bu(t), \\ & F(t) = \hat{\theta}(z(t) - z_{\text{ref}}(t)) + \hat{\theta}_0, \\ & d(t+1) = d(t) + K_d F(t) \left\| \begin{bmatrix} x(t+1) \\ y(t+1) \end{bmatrix} - \begin{bmatrix} x(t) \\ y(t) \end{bmatrix} \right\|_2 \\ & W(t) = \max(\alpha(t) \sin(\psi(t)), \beta(t) \cos(\psi(t))), \\ & \alpha(t) = \frac{2m\sqrt{1+a^2}d(t)}{m^2 - a^2}, \beta(t) = \frac{2d(t)}{\sqrt{m^2 - a^2}}, \\ & \bar{x}(t) \in \mathcal{X}, u(t) \in \mathcal{U}, t = 0, 1, \dots, (N-1), \\ & s(0) = s_0, \bar{x}(0) = \bar{x}_0, \end{aligned} \quad (13)$$

where $s(t) = [x(t), y(t), W(t)]^T$, $Q \succ 0$, and s_0, \bar{x}_0 are known and fixed. After computing the optimal trajectory, we apply the whole batch solution, $U_t = [u(0), u(1), \dots, u(N-1)]$, as an open loop rollout without re-solving (13) during the stroke. We then use an image of the drawn stroke to estimate the actual width $W_a(\zeta(t)) := W_a(t)$ along the generated stroke. The computation of this actual width is detailed in Section 5. The actual and the reference stroke widths are then compared to compute an *error metric* as:

$$V = \sum_{t=0}^N |W_a(t) - W_{\text{ref}}(t)|. \quad (14)$$

Note that the reference width $W_{\text{ref}}(t)$ is computed along the reference position trajectory for all t . Thus, the error metric in (14) is only concerned with quantifying the z -direction force tracking error and not x, y tracking. The x, y position tracking error is regulated by tuning matrix Q and the low level control parameters of the robot. We do not apply learning for such control loop.

5. EXPERIMENTAL RESULTS

In this section we present detailed experimental results with our proposed theory. We first show the efficacy of the offline model fitting strategy presented in Section 4.1, but then also highlight the iterative lowering of error metric (14) if the model parameters in (6) are learned after iterative stroke attempts via (13). Such iterative learning attempts also offer an intuitive bound for T_{off} .

5.1 Hardware Setup

We perform the real-world experiments using a UR5e 6-DOF manipulator with a custom end-effector that is holding the drawing utensil. The tool is rigidly mounted, as shown in Fig. 1, which imposes a hard constraint on the maximum allowable force applied by the robot arm when drawing. We use a Logitech Brio 4K Webcam to capture images of the drawings.

5.2 Image Processing and Computing $W_a(t)$

In order to evaluate the closed-loop error metric of a stroke as defined in (14), we use images of the performed stroke and compare them to a desired one. In this case, we start with a desired (i.e., reference) stroke generated from a parametric curve (1). The first sequence is performed with a nominal open loop maneuver that is pre-selected. After the robot performs the stroke, the robot takes an image with the camera. The color image is converted to grayscale and then a threshold filter is applied based on the darkness of the actual stroke and the canvas. Finally, a contour filter is used to detect the stroke outline. Starting at the known beginning of the stroke and following along the parametric curve, we compute the width at each sampled point by finding the closest points which are perpendicular to the tangent line. This lets us compute the error metric (14).

5.3 Offline Force Calibration and Model Fitting

To learn the parameters in model (6), we took measurements using the force sensor on the UR5e as the robot moved the tool downwards into the work surface. We ran sinusoidal sweeps of various penetration depths and used linear regression to determine the applied force as a function of penetration depth. Fig. 4 shows the line of best

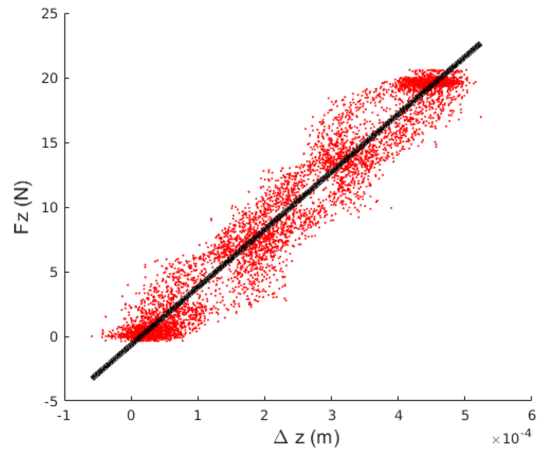


Fig. 4. Force vs penetration plot.

fit plotted on top of the force measurements vs penetration depths. Due to the work surface not being flat, we recorded the contact points along the x and y directions shown in Fig. 8. The height of the contact points are used as offsets to z_{ref} to maintain a consistent penetration depth along a stroke after contact is initially made during a trial.

Thus, parameters of (6) can be learned offline as shown in Fig. 8. However, in the next two sections, in order

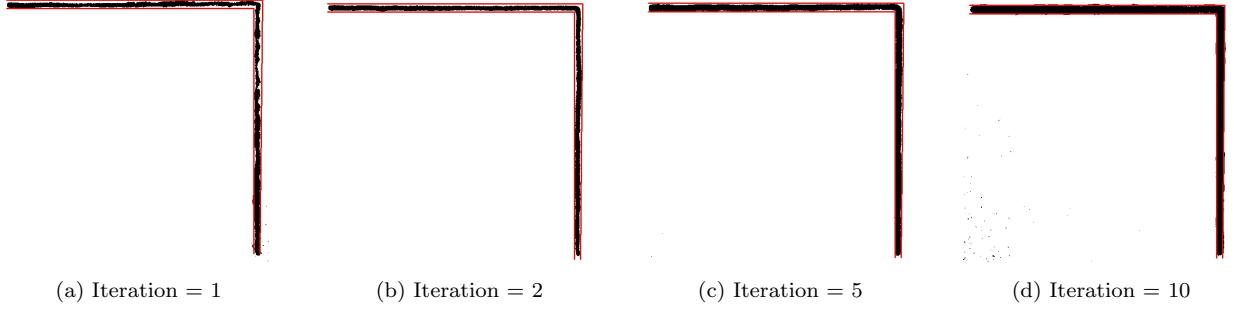


Fig. 5. Post-processed images of pencil strokes with $\gamma = 0^\circ$

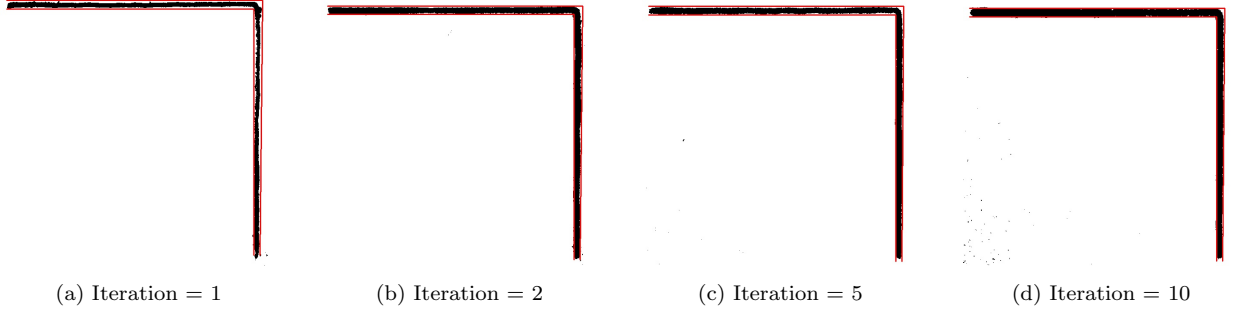


Fig. 6. Post-processed images of pencil strokes with $\gamma = 50^\circ$

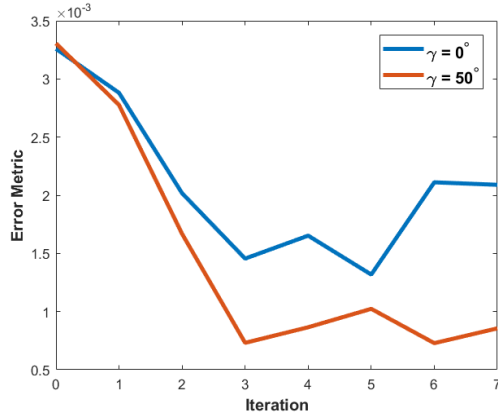


Fig. 7. Comparison of the error metric with standard ($\gamma = 0^\circ$) vs our approach ($\gamma = 50^\circ$).

to demonstrate an iterative improvement of the stroke starting from the same initial condition, instead of offline fitting as shown in Section 4.1 and Fig. 8, we learn the model parameters in (6) after every iterative attempt of the stroke obtained through a solution of (13). Note, each stroke is independent, and not drawn over the previous.

5.4 Deposition with Degradation

We set the baseline for comparison as a pencil that is mounted perpendicular to the work surface, similar to [Adamik et al., 2022, O’Dowd, 2019], where $\gamma = 0^\circ$ and initial tip width, $\alpha(0) = \beta(0)$, as 0.1mm. The robot performs a stroke where the desired width is 1.0mm as it moves right and 0.7mm as it moves down as seen in Fig. 5. We repeat these trials using an angled pencil where $\gamma = 50^\circ$, $m = 5.45$, $d_0 = 0.1$ mm. Fig. 7 shows our approach using an angled pencil outperforms the baseline throughout the iterations with error metric lowered by

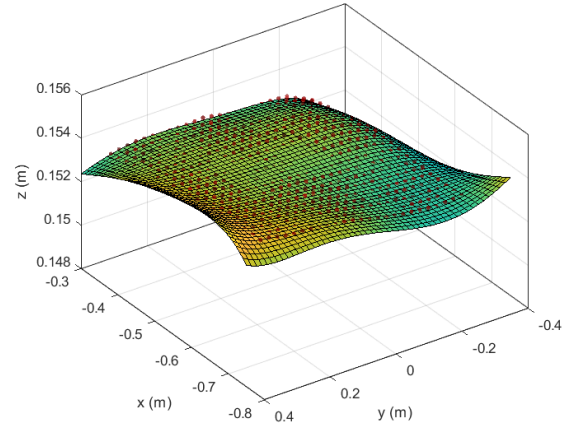


Fig. 8. Surface plot of contact points on the drawing table.

about 3.6% all the way to 65.5%. A main reason for this is the ability to vary the deposition width by controlling the ψ of the pencil while it is tilted. A pencil with $\gamma = 0^\circ$ can only have a single width since the surface of the tip that makes contact with the paper is a circle. This can be a problem as seen in iteration 10 where the tip becomes larger than desired and there is no way to correct it. Our approach can also decrease the number of strokes necessary to draw a picture that requires shading since it can leverage the longer diameter while still doing precise strokes with the shorter minor axis diameter.

6. CONCLUSION

We presented a data-driven optimization approach for robot controlled deposition with a degradable tool, specifically the robotic drawing problem. We utilized visual and force feedback to update the unknown model parameters of our tool-tip using least squares. We solved a constrained finite time optimal control problem for tracking the refer-

ence deposition profile, where our robot planned with the learned tool degradation dynamics. With real experiments on a UR5 robot, we showed that the error in target vs actual deposition decreased by up to 65% due to the incorporation of learned degradation models in our trials.

REFERENCES

- Adamik, M., Goga, J., Pavlovicova, J., Babinec, A., and Sekaj, I. (2022). Fast robotic pencil drawing based on image evolution by means of genetic algorithm. *Robotics and Autonomous Systems*, 148, 103912. doi:https://doi.org/10.1016/j.robot.2021.103912.
- Avigal, Y., Berscheid, L., Asfour, T., Kröger, T., and Goldberg, K. (2022). Speedfolding: Learning efficient bimanual folding of garments.
- Bidgoli, A., De Guevara, M.L., Hsiung, C., Oh, J., and Kang, E. (2020). Artistic Style in Robotic Painting; A Machine Learning Approach to Learning Brushstroke from Human Artists. *29th IEEE International Conference on Robot and Human Interactive Communication, RO-MAN 2020*, 412–418. doi:10.1109/RO-MAN47096.2020.9223533.
- Brown, T.B., Mann, B., Ryder, N., Subbiah, M., Kaplan, J., Dhariwal, P., Neelakantan, A., Shyam, P., Sastry, G., Askell, A., Agarwal, S., Herbert-Voss, A., Krueger, G., Henighan, T., Child, R., Ramesh, A., Ziegler, D.M., Wu, J., Winter, C., Hesse, C., Chen, M., Sigler, E., Litwin, M., Gray, S., Chess, B., Clark, J., Berner, C., McCandlish, S., Radford, A., Sutskever, I., and Amodei, D. (2020). Language models are few-shot learners. *Advances in Neural Information Processing Systems*, 2020-December.
- Cao, N., Yan, X., Shi, Y., and Chen, C. (2019). AI-Sketcher: A deep generative model for producing high-quality sketches. *33rd AAAI Conference on Artificial Intelligence, AAAI 2019, 31st Innovative Applications of Artificial Intelligence Conference, IAAI 2019 and the 9th AAAI Symposium on Educational Advances in Artificial Intelligence, EAAI 2019*, 2564–2571. doi:10.1609/aaai.v33i01.33012564.
- Deng, J., Dong, W., Socher, R., Li, L.J., Li, K., and Fei-Fei, L. (2009). Imagenet: A large-scale hierarchical image database. In *2009 IEEE Conference on Computer Vision and Pattern Recognition*, 248–255. doi:10.1109/CVPR.2009.5206848.
- Ebert, F., Yang, Y., Schmeckpeper, K., Bucher, B., Georgakis, G., Daniilidis, K., Finn, C., and Levine, S. (2022). Bridge Data: Boosting Generalization of Robotic Skills with Cross-Domain Datasets. 2–8. doi:10.15607/rss.2022.xviii.063.
- Gao, F., Zhu, J., Yu, Z., Li, P., and Wang, T. (2020). Making robots draw a vivid portrait in two minutes. *IEEE International Conference on Intelligent Robots and Systems*, 9585–9591. doi:10.1109/IROS45743.2020.9340940.
- Huang, Z., Zhou, S., and Heng, W. (2019). Learning to paint with model-based deep reinforcement learning. *Proceedings of the IEEE International Conference on Computer Vision*, 2019-October, 8708–8717. doi:10.1109/ICCV.2019.00880.
- Jain, S., Gupta, P., Kumar, V., and Sharma, K. (2015). A force-controlled portrait drawing robot. *Proceedings of the IEEE International Conference on Industrial Technology*, 2015-June(June), 3160–3165. doi:10.1109/ICIT.2015.7125564.
- Kotani, A. and Tellex, S. (2019). Teaching robots to draw. *Proceedings - IEEE International Conference on Robotics and Automation*, 2019-May, 4797–4803. doi:10.1109/ICRA.2019.8793484.
- Lam, J.H. and Yam, Y. (2009). Stroke trajectory generation experiment for a robotic Chinese calligrapher using a geometric brush footprint model. *2009 IEEE/RSJ International Conference on Intelligent Robots and Systems, IROS 2009*, 1, 2315–2320. doi:10.1109/IROS.2009.5354709.
- Leidner, D., Bejjani, W., Albu-Schäffer, A., and Beetz, M. (2016). Robotic agents representing, reasoning, and executing wiping tasks for daily household chores. *Proceedings of the International Joint Conference on Autonomous Agents and Multiagent Systems, AAMAS*, (Aamas), 1006–1014.
- O’Dowd, P.J. (2019). A robot that draws and shades with tactile force feedback sensed through a pencil. In *EVA*.
- Ramesh, A., Dhariwal, P., Nichol, A., Chu, C., and Chen, M. (2022). Hierarchical text-conditional image generation with clip latents.
- Ramesh, A., Pavlov, M., Goh, G., Gray, S., Voss, C., Radford, A., Chen, M., and Sutskever, I. (2021). Zero-shot text-to-image generation.
- Rombach, R., Blattmann, A., Lorenz, D., Esser, P., and Ommer, B. (2022). High-Resolution Image Synthesis with Latent Diffusion Models. 10674–10685. doi:10.1109/cvpr52688.2022.01042.
- Saharia, C., Chan, W., Saxena, S., Li, L., Whang, J., Denton, E., Ghasemipour, S.K.S., Ayan, B.K., Mahdavi, S.S., Lopes, R.G., Salimans, T., Ho, J., Fleet, D.J., and Norouzi, M. (2022). Photorealistic text-to-image diffusion models with deep language understanding.
- Song, D., Lee, T., and Kim, Y.J. (2018). Artistic pen drawing on an arbitrary surface using an impedance-controlled robot. *Proceedings - IEEE International Conference on Robotics and Automation*, 4085–4090. doi:10.1109/ICRA.2018.8461084.
- Suomalainen, M., Karayiannidis, Y., and Kyrki, V. (2022). A survey of robot manipulation in contact. *Robotics and Autonomous Systems*, 156, 1–57. doi:10.1016/j.robot.2022.104224.
- Tong, Z., Chen, X., Ni, B., and Wang, X. (2021). Sketch Generation with Drawing Process Guided by Vector Flow and Grayscale. *35th AAAI Conference on Artificial Intelligence, AAAI 2021*, 1(Dodson), 609–616. doi:10.1609/aaai.v35i1.16140.
- Villegas, R., Babaeizadeh, M., Kindermans, P.J., Moraldo, H., Zhang, H., Saffar, M.T., Castro, S., Kunze, J., and Erhan, D. (2022). Phenaki: Variable length video generation from open domain textual description.
- Wang, S., Chen, J., Deng, X., Hutchinson, S., and Dellaert, F. (2020). Robot calligraphy using pseudospectral optimal control in conjunction with a novel dynamic brush model. *IEEE International Conference on Intelligent Robots and Systems*, 6696–6703. doi:10.1109/IROS45743.2020.9341787.
- Xie, N., Hachiya, H., and Sugiyama, M. (2013). Artist agent: A reinforcement learning approach to automatic stroke generation in oriental ink painting. *IEICE Transactions on Information and Systems*, E96-D(5), 1134–1144. doi:10.1587/transinf.E96.D.1134.